Neutron Reflectivity Study of End-Adsorbed Bimodal Polymer Systems under Static Conditions and Shear Flow

ARTICLE *in* MACROMOLECULES · AUGUST 2013

Impact Factor: 5.8 · DOI: 10.1021/ma401011f

6 AUTHORS, INCLUDING:

Nikolaos Spiliopoulos

University of Patras

25 PUBLICATIONS **242** CITATIONS

SEE PROFILE

Alexandros Vradis

University of Patras

33 PUBLICATIONS **260** CITATIONS

SEE PROFILE

Macromolecules

Article

pubs.acs.org/Macromolecules

Neutron Reflectivity Study of End-Adsorbed Bimodal Polymer Systems under Static Conditions and Shear Flow

Dimitrios L. Anastassopoulos,[†] Nikolaos Spiliopoulos,[†] Alexandros A. Vradis,[†] Chris Toprakcioglu,*[,†] Allain Menelle,[‡] and Fabrice Cousin[‡]

[†]Department of Physics, University of Patras, GR 26 504 Patras, Greece

[‡]Laboratoire Léon Brillouin, CEA Saclay, Gif sur Yvette 91191, Cedex, France

ABSTRACT: The behavior of end-adsorbed bimodal PS−PEO block copolymer systems was studied with neutron reflectivity experiments, both under static conditions (zero shear rate) and under a stepwise-increasing shear flow, up to a critical shear rate where desorption occurs. It is found that when the height of one kind of chain in the bimodal brush is significantly greater than that of the other, the longer chains desorb first, while if the heights of the two constituent kinds of chains in the brush are similar, then the bimodal system responds as a whole and both kinds of chain desorb simultaneously. In particular, when the chain height ratio of the two components of the bimodal system is less than 0.80, the reflectivity spectra under static conditions are best fitted by two parabolas, and under shear flow each component desorbs at a different shear rate. Above this value, the bimodal system reacts en bloc, and desorption occurs at the same shear rate for both copolymers. It is further observed that the critical shear rate for desorption, in all bimodal systems studied in the present investigation, scales with s^{-3}, where s is the mean interanchor distance, in accord with the behavior of monodisperse brushes reported previously [Anastassopoulos et al. *Macromolecules* **2006**, *39*, 8901−8904]. In addition, careful measurements under shear flow up to and in the vicinity of the critical shear rate for desorption show no evidence of any measurable change in the brush height or volume fraction profile.

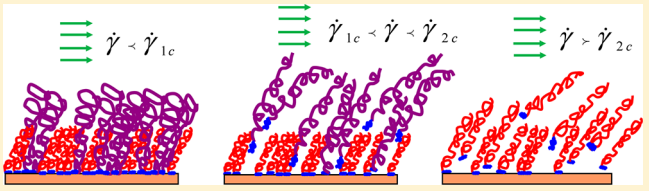

INTRODUCTION

Polymer brushes, consisting of same-length chains (monodisperse brushes), adsorbed on solid−liquid or liquid−air interface, have important physical properties for many practical applications, such as lubrication, wetting, adhesion, and stabilization of colloidal dispersions.[1] A large volume of work, both experimental and theoretical, has been carried out in the past three decades for these systems.[2−15]

While much of this work corresponds to monodisperse systems, in practice there may be situations where the end-tethered chains are polydisperse or the brush systems consists of two or more different polymeric species. Such systems offer increased versatility in surface modification, particularly when it is desirable to tune the response of the brush to external stimuli such as solvent quality or pH.[16]

Bimodal brushes composed of chains of two different chain lengths provide an interesting framework both from a theoretical viewpoint and in terms of optimizing the physical properties of the system due to the formation on the interface of a more complex polymeric layer, whereby the response of the two components to the brush environment may be different. These systems have been studied by analytic self-consistent-field (SCF) theory,[17−19] by numerical self-consistent models,[20] by computer simulation models,[21,22] and experimentally by neutron reflectivity.[23]

The behavior of polymer chains tethered to a surface under conditions of shear has been examined in a number of works, both by theory or simulation[24−33] and experimentally.[9,34,35] The response of such chains to shear has numerous technological implications on dispersion stability, rheology, lubrication, and related areas.

In our previous studies,[34,35] we have used neutron reflectometry to investigate end-adsorbed polystyrene brushes exposed to shear flow in good solvent. We have found that the brush volume fraction profiles show no evidence of change with increasing shear rate until a critical shear rate threshold $\dot{\gamma}_c$ is reached, above which a discontinuous transition in desorption rate takes place. It was observed that this threshold depends on the brush interchain anchoring distance s and that it increases with s^{-3} .

In the present work we have extended our previous results by studying bimodal polymer brushes under different shear rates. Bimodal layers were prepared by using two diblock copolymers of PS−PEO with different molecular weights of PS. The PS−PEO copolymers were highly asymmetric, with a large PS dangling block and a much smaller PEO anchoring block. The behavior of five bimodal systems has been examined with neutron reflectivity experiments, both under static conditions (zero shear)and under various applied shear rates, aiming to examine the behavior of each component under shear flow in the presence of the other.

Received: May 15, 2013
Revised: July 27, 2013
Published: August 29, 2013

More specifically, we wished to investigate whether the bimodal brush desorbs at some critical shear rate like its unimodal counterpart and if so at what value of this critical shear rate. In particular, the question arises whether the two different molecular weight chains comprising the bimodal brush desorb simultaneously or require different values of critical shear rate to do so. Furthermore, it would be important to find out if any observed desorption obeys the s^{-3} law that has been previously established for single polymer solutions.[35] Finally, in view of earlier reports of brush swelling under shear[36,37] and the long-standing question regarding the possibility of shear-induced expansion of polymer brushes, it would be of considerable interest to confirm our previous experimental observation[35] that just below the critical value of shear rate, $\dot{\gamma}_c$, where detachment occurs, the polymer brush shows no evidence of swelling.

In the only simulation work in the literature[38] dealing with bimodal brushes in shear, the method of self-consistent Brownian dynamics has been adapted to simulate the properties of bimodal polymer brushes under shear. Under very strong shear rates the authors report collapse of the bimodal brush due to the fact that the long chains are compressed. No desorption has been reported.

NEUTRON REFLECTOMETRY AND DATA ANALYSIS

The bimodal systems we used consist of end-adsorbed macromolecular chains of two different molecular weights of a highly asymmetric block copolymer polystyrene-*b*-poly(ethylene oxide) (PS−PEO) under good solvent conditions. A bimodal brush is thus formed, where the shorter PEO blocks anchor the chains onto a quartz substrate from toluene solution. This diblock copolymer has been extensively studied and characterized by numerous techniques.[8,11]

The block copolymers used in the present work were obtained from Polymer Laboratories Ltd., and their molecular characteristics have been presented elsewhere.[35] The studied pairs of polymers for the formation of the bimodal system are shown in Table 1.

For the selection of the constituent polymers of the bimodal brush the following considerations have been taken into account:

Table 1. Experimental Characteristics of Bimodal Systems under Static Conditions

bimodal system	ratio of initial solution concn[a] (mg/mL)	heights of brushes[b] (Å)	ratio of chain heights	no. of parabolas for best fitting
50K−80K	0.05:0.05	300(±15):520	0.58	2
80K−182K	0.05:0.05	500:760	0.66	2
80K−239K	0.05:0.10	460:810	0.57	2
182K−322K	0.05:0.05	760:850	0.89	1 or 2[c]
182K−239K	0.05:0.05	760:810	0.94	1 or 2[c]

[a]Refers to the concentration of block copolymer in toluene solution in which adsorption took place. [b]Refers to the height of each brush component in the bimodal brush as determined by fitting the neutron reflectivity profile to a two-parabola model or to a single parabola model, as indicated in last column of Table 1 [c]For this system, both the single parabola plus Gaussian tail and the two-parabola models gave an equally good fit.

First, the polymers should have similar affinity to the surface in order to ensure a satisfactory level of adsorption for each one of them. For this reason, pairs of polymers with large deviations in molecular weights have been avoided. At the same time, however, we tried to vary the ratio of brush height of the two polymers as widely as possible. As can be seen in Table 1, the height ratio for the five used pairs varied from 0.55 to 0.95.

Brush heights were determined through the volume fraction profiles. The concentration ratio of the two polymers in solution was kept in almost all cases to a value of 1:1 (see Table 1).

Solutions in *d*-toluene at a concentration of 0.05 mg/mL for each PS−PEO block copolymer constituent were used. Adsorption took place on optically flat quartz slabs of dimensions 50 mm × 100 mm × 12 mm over a period of 12 h.

Before adsorption of the block copolymers the quartz substrates were cleaned in 3:1 (v/v) H_2SO_4−HNO_3 followed by 3:1 (v/v) HCl−HNO_3 for 6 h each. Then, the substrates were washed in distilled water followed by a rinse with absolute ethanol and were allowed to dry.

Reflectivity measurements were taken with the aid of a Teflon cell described in detail elsewhere.[39] The cell, which contains the polymer solution and the optically flat quartz slab as substrate, allows laminar flow of solvent through adjustable gaps in the range of 0.2−1.0 mm in plane Poiseuille geometry and at shear rates ranging from 10 to 60 × 10^3 s^{-1}. The shear rate at the solid−liquid interface is calculated from the measured flow rate assuming a parabolic velocity profile. A neutron beam is allowed to enter the quartz plate from its side and is reflected from the quartz/*d*-toluene interface, where the polymer is adsorbed.

Neutron reflectivity measurements were obtained using the EROS time-of-flight spectrometer at the Laboratoire Leon Brillouin in Saclay.[40] The angle of incidence, θ, was 0.75 °, and the wavelength was in the range of 2−30 Å. The reflectivity was measured as a function of the scattering vector $\vec{Q}$, whose magnitude is given by $Q = (4\pi/\lambda) \sin \theta$.

In order to fit the neutron reflectivity data from adsorbed bimodal polymer systems, the Simplex method was used as a fitting routine to minimize the sum of the weighted squared differences between the experimental points and the fitted reflectivity curves with respect to the fitting parameters.

Provided that sufficient data are collected so that the statistical error of the measurements is kept low (as is the case in this study and other investigations[34,35,41,42]), neutron reflectometry[43] is a very sensitive probe of the volume fraction profile of adsorbed or grafted macromolecular species. This sensitivity is needed to detect both the detachment of a component in a bimodal system and the possibility of swelling of the polymer brush when shear flow is applied. Both effects are analyzed later in this work.

Static Experiments. The behavior of the bimodal systems was first studied without application of shear flow (static experiments).

In Figure 1, neutron reflectivity for the bimodal system 50K−80K is presented. Reflectivity is multiplied by Q^4 in order to intensify the differences between experimental points and fitted curves. Two fitted curves are shown together with experimental points (open circles). The continuous curve corresponds to fitting using two parabolas while the dotted curve relates to one parabolic profile together with a Gaussian tail.

From Figure 1, it is concluded that best fitting is achieved by the two-parabola approach as the dotted curve misses several

dx.doi.org/10.1021/ma401011f | Macromolecules 2013, 46, 6972−6980

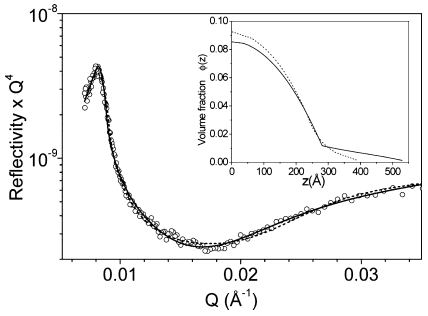

Figure 1. Reflectivity profile of bimodal 50K−80K PS−PEO diblock copolymer brush at zero shear flow (○). Reflectivity is multiplied by Q^4 in order to enhance the difference between the two different fits. The best fit is achieved by a two-parabola model (continuous line) as described in the text. The dotted line which corresponds to fitting with a single parabola with a Gaussian tail misses numerous experimental points. Inset: best-fit volume fraction profile for bimodal 50K−80K PS−PEO diblock copolymer brush. The two-parabola fit (continuous line) is better than the corresponding fit obtained from the one-parabola with Gaussian tail model (dotted line).

experimental points, as for example, in the region around Q = 0.02 Å^{-1}. This is also confirmed by numerical comparison of the fitting quality which gives a 40% smaller sum in the squared deviations in the case of two parabolas compared to the single one with a tail.

Volume fraction profiles for the static measurement on the 50K−80K system are shown in the inset of Figure 1. Again, the continuous curve corresponds to the two-parabola model while the dotted curve depicts the one parabola plus a Gaussian tail model. From the above profiles the corresponding length ratio of the two brushes is calculated to be 0.58 (Table 1).

Similar results were obtained in the case of the 80K−182K and 80K−239K bimodal systems. Both reflectivity spectra from these systems are much better fitted by the two-parabola model compared to the single one. In the case of the double-parabola model, the sum of the squared deviations is found to be smaller, by at least 20%, compared to the single parabola plus a Gaussian tail approximation.

However, it is very interesting to note that in the case of 182K−239K and 182K−322K this situation is different. For these bimodal systems, the reflectivity spectra are fitted equally well both by one parabola with a Gaussian tail and by the double-parabola model. In Figure 2, the volume fraction profile for the bimodal system 182K−322K is shown, where the dotted line is the fitting result using the one-parabola model together with a Gaussian tail and the continuous line is the result obtained with the double-parabola model. Numerical calculation shows that both fits are equally satisfactory. So in the reflectivity spectrum (not shown) there is no distinguishable difference between the curves from the above volume fractions.

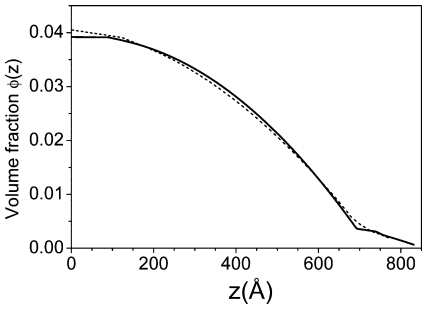

Figure 2. Volume fraction profiles for static reflectivity data of 182K−322K bimodal block copolymer brush. The continuous line is the best fit using the two-parabola model while the dotted line is the best fit obtained with one parabola with a Gaussian tail. Both volume fraction profiles give equally satisfactory fits to experimental reflectivity profile.

From these findings it is concluded (see also Table 1) that when the length ratio of the bimodal components is less than 0.80, then the reflectivity spectrum is best approximated by a double parabolic volume fraction profile. On the contrary, when the bimodal systems are formed from components similar in length, then the reflectivity spectrum can just as well be approximated by a single parabolic volume fraction profile with a small Gaussian tail.

Application of Shear Flow. For each of the bimodal systems in Table 1, after measuring the static reflectivity spectra, a series of reflectivity profiles were measured by increasing the shear rate in small steps. The results of these experiments are summarized in Table 2. It is known from previous studies on unimodal brushes[35] that PS−PEO block copolymers undergo rapid desorption from quartz when the shear rate exceeds a certain threshold. In the present study, desorption from the quartz surface has been observed for all five bimodal systems. For three of them each component desorbs under a different shear rate, while for the other two cases, desorption occurs simultaneously (i.e., at the same shear rate). It is worth noting that starting from static conditions until the time of strong shear flow, where detachment of the polymer brush occurs, there is no measurable change in the brush height.

Figure 3 shows the reflectivity spectrum for the bimodal system 50K−80K, both static and under a shear rate 7050 s^{-1}, where desorption of the high molecular weight component (80K) has been observed. In the inset of Figure 3 the volume fraction profiles for this bimodal system are shown. For the static case, best fit is achieved by a two-parabola profile, as explained above, while the profile of the residual polymer after desorption is fitted by a parabola with a brush height of 300 Å. This fact is fully consistent with the notion that only the 50K polymer remains adsorbed on the surface since this is exactly the brush height one would expect for this polymer.

Figure 4 shows the change in adsorbance of 50K−80K bimodal system as a function of increasing shear rate. Note that each experimental point in this figure corresponds to a reflectivity spectrum accumulated over a period of 3 h.

From the change of 0.63 mg/m^2 (Table 2), which occurred at 7050 s^{-1}, the average interanchor distance for the 80K component has been calculated. The values of $\dot{\gamma}_c$ obtained are in accordance with the power law $\dot{\gamma}_c \sim s^{-3.35}$.

Similarly, reflectivity spectra from the 80K−239K bimodal are shown in Figure 5, both for the static case and under a shear rate of 672 s^{-1}, where desorption of the 239K polymer is observed. It should be noted that in this case, due to the large difference in the molecular weight of the two polymers and the inferior affinity of the 239K to the surface, the concentration ratio of 80K over 239K in the solution was kept to 1:2 in order to ensure satisfactory adsorption of the higher molecular weight polymer.

As mentioned above, the static reflectivity curve of this system is best fitted by the two-parabola profile. The parabolic profile corresponding to 239K reaches up to 800 Å (inset of Figure 5) and corresponds to an adsorbance as little as 0.35 mg/m^2, which is exactly the desorbed polymer quantity at the

dx.doi.org/10.1021/ma401011f | Macromolecules 2013, 46, 6972−6980

Table 2. Experimental Characteristics of Bimodal Brush Systems under Shear Flow[a]

bimodal system	Γ (mg/m^2) static	s (Å)	$\dot{\gamma}_c$ (s^{-1})	Γ (mg/m^2) after 1st desorption	s (Å)	$\dot{\gamma}_c$ (s^{-1})	Γ (mg/m^2) after 2nd desorption
50K−80K	1.85	145 (80K)	7050	1.22			
80K−182K	2.00	246 (182K)	1500	1.50	94 (80K)	24500	0.1
80K−239K	2.65	337 (239K)	672	2.30			
182K−322K	1.90	132	9450	0.05			
182K−239K	2.40	121	12852	0.17			

[a]Bimodal systems (column 1). Initial adsorbance Γ for each system at zero shear rate (column 2). Interchain spacing s of desorbed chains (their molecular weight is indicated in parentheses) and critical shear rate $\dot{\gamma}_c$ (columns 3 and 4, respectively). Adsorbance Γ after the first desorption (column 5). Interchain spacing s of desorbed chains and critical shear rate $\dot{\gamma}_c$ for the remaining component (80K) of the 80K−182K bimodal system (columns 6 and 7, respectively).

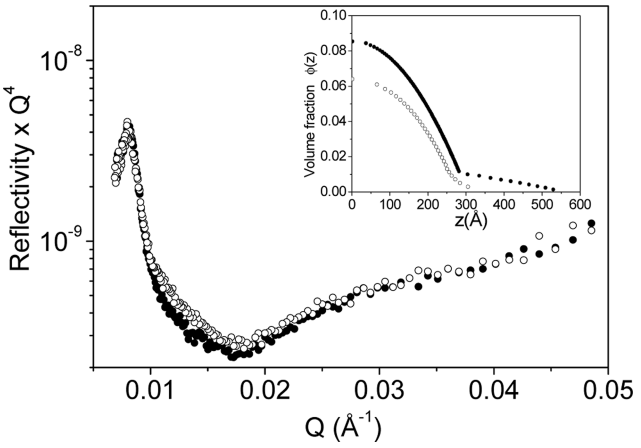

Figure 3. Reflectivity profile of bimodal 50K−80K PS−PEO diblock copolymer brush. Filled circles represent the static (zero shear) experimental profile with total adsorbance 1.85 mg/m^2. Open circles depict the profile after 80K PS−PEO desorption at 7050 s^{-1} with remaining adsorbance 1.22 mg/m^2. Inset: volume fraction profiles for above-described reflectivity profiles. Filled circles represent the volume fraction profile obtained from the best fit to the static (zero shear) reflectivity profile using the two-parabola model while open circles correspond to the profile after the desorption of 80K PS−PEO at 7050 s^{-1}.

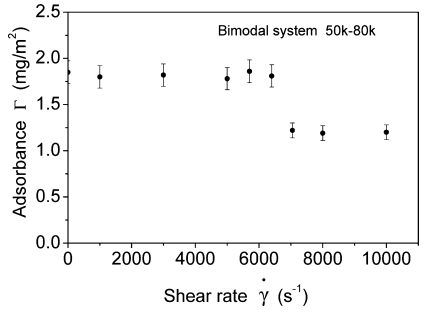

Figure 4. Change of adsorbance values for 50K−80K PS−PEO brush bimodal system. Each point is calculated from the area under the volume fraction profile determined at each shear rate. Desorption of the 80K PS−PEO component occurs at 7050 s^{-1}.

shear rate of 672 s^{-1} (Figure 5). Although the desorbed quantity is small, the change in the reflectivity spectra is clearly noticeable.

The reflectivity spectrum after desorption at 672 s^{-1} (Figure 5, open circles) is fitted very well by a single parabola (inset of Figure 5, open circles) corresponding to a brush height of about 500 Å, implying that only the 80K polymer remains on the surface.

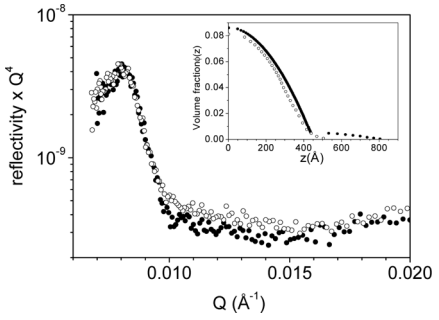

Figure 5. Reflectivity profile of bimodal 80K−239K PS−PEO diblock copolymer brush. Filled circles represent the measured static (zero shear) reflectivity profile while open circles indicate the profile after desorption of the 239K PS−PEO component of the brush at 672 s^{-1}. Inset: volume fraction profiles for above-described reflectivity profiles. Filled circles represent the volume fraction profile obtained from the best fit to the static (zero shear) reflectivity profile using the two-parabola model while open circles show the profile after the desorption of 239K PS−PEO at 672 s^{-1}.

The change of adsorbance with shear rate for the bimodal system 80K−239K is shown in Figure 6. The interanchor

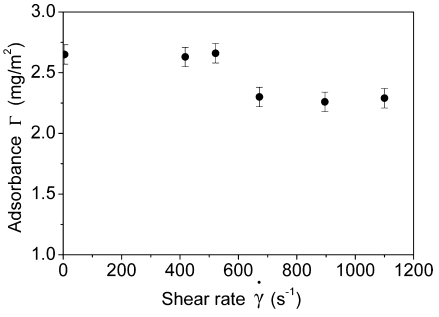

Figure 6. Change of adsorbance with shear rate for the 80K−239K PS−PEO bimodal brush system. Each point is calculated from the area under the volume fraction profile determined at each shear rate. Desorption of 239K PS−PEO component occurs at 672 s^{-1}.

distance corresponding to 0.35 mg/m^2 for the 239K component is 337 Å, which, together with the measured value of 672 s^{-1} for the critical shear rate for desorption, is again in accord with the $\dot{\gamma}_c \sim s^{-3}$ power law.

For these two bimodal brushes, however, it was not possible to observe desorption for both components in one experiment. The reason is that when a single polymer of high molecular weight is adsorbed, the critical shear rate for desorption depends on the interanchor distance according to the s^{-3} law.[35] If this distance is large enough, desorption occurs at relatively low shear rates. In the presence of a second polymer of smaller

dx.doi.org/10.1021/ma401011f | Macromolecules 2013, 46, 6972−6980

molecular weight, the interanchor distance between the chains of the larger brush increases and detachment of this polymer requires an even smaller shear rate.

As described in the experimental section, the shear rate in our setup is controlled by the pumping speed and the gap between a Teflon block and the quartz crystal. The lowest possible pumping speed sets a lower limit to the achievable shear rate, and any further reduction is only possible by increasing the gap.

On the other hand, detachment of the remaining smaller molecular weight component would now require a considerably higher shear rate. However, if the pumping speed is increased too much, the flow would not be laminar any more, as the Reynolds number would by far exceed the value of 1000, so a reduction of the gap is necessary. Starting with a rather large gap, detachment of both polymers has been achieved only in the case of molecular weights 80K−182K in the following way:

After the first observed change relative to the static reflectivity spectrum at a shear rate of 1500 s^{-1}, which is attributed to the detachment of the higher molecular weight polymer (182K), the spectrum was monitored in order to ensure its stability for about 3 h (Figure 7, open circles). During this period no significant change was observed under this shear rate.

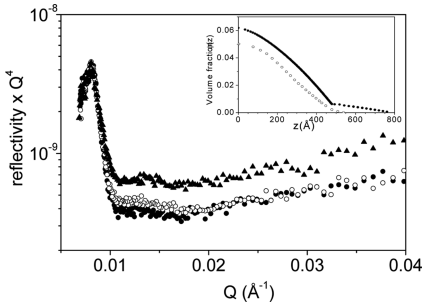

Figure 7. Reflectivity profile of bimodal 80K−182K PS−PEO diblock copolymer brush. Filled circles represent the experimental points of the static (zero shear) profile. Open circles depict the profile after desorption of the 182K PS−PEO component at 1500 s^{-1}, while triangles show the reflectivity profile after 80K PS−PEO desorption at 24 500 s^{-1}. At 24 500 s^{-1} almost all of the bimodal system is found to have detached from the surface. Inset: volume fraction profiles for above-described reflectivity profiles. Filled circles indicate the volume fraction profile obtained from the best fit to the static (zero shear) reflectivity profile using the two-parabola model. Open circles correspond to the volume fraction profile after 182K PS−PEO desorption.

Then the cell was emptied, and the O-ring, adjusting the gap between the quartz plate and the Teflon block, was changed for a thinner one. This changed the gap from 0.65 to 0.25 mm. In this way the shear rate could be increased by a factor of about 7 under the same flow rate. Then the cell was assembled again and a static neutron reflectivity measurement was taken. The measured spectrum was identical to the one measured after the detachment of the higher molecular weight polymer. This result indicates that no measurable readsorption of the 182K polymer has occurred within the time scale of the reflectivity measurement (ca. 1.5 h). This is reasonable because much longer times are likely required for the readsorption of the 182K polymer onto a substrate that already bears the 80K brush, since the presence of this brush constitutes a kinetic barrier to in-coming 182K chains and slows down the adsorption kinetics considerably.

By a quick curve-fitting procedure, before applying any shear flow, the remaining polymer quantity, which presumably corresponds to the lower molecular weight polymer (80K), was estimated. From this estimated value of adsorbance, the shear rate for detachment of the second polymer was calculated from the s^{-3} power low. Then reflectivity measurements were taken with increasing shear rates (by increasing the flow rate) so as to approach the calculated shear rate threshold for detachment of the remaining polymer. Further detachment was observed at a shear rate of 24 500 s^{-1} (Figure 7, black triangles).

Two volume fraction profiles, corresponding to reflectivity spectra of the bimodal system 80K−182K of Figure 7, are shown in inset of Figure 7. The static profile is best fitted by two parabolas (black circles). After detachment of the 182K polymer at a shear rate of 1500 s^{-1}, the profile is approximated by one parabola which corresponds to the 80K remaining polymer with a brush height of 500 Å. The adsorbance versus the applied shear rate for the bimodal system 80K−182K is shown in Figure 8. The critical shear rates for desorption of this bimodal system are included in Table 2 and are also in accord with the $\dot{\gamma}_c \sim s^{-3}$ power law.

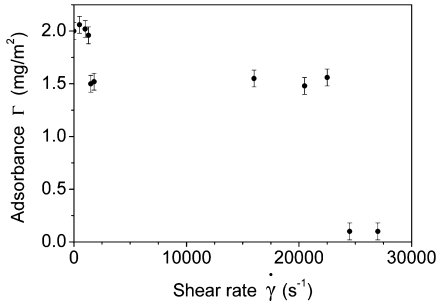

Figure 8. Adsorbance values of 80K−182K PS−PEO bimodal brush system. The desorption of the 182K PS−PEO component took place at 1500 s^{-1}. The remaining 80K PS−PEO component desorbs at 24 500 s^{-1}.

A very detailed study was carried out for the 182K−322K bimodal system, whereby following the static measurement, the reflectivity profiles were measured for a large number of different shear rates using a small incremental increase in shear rate particularly in the region of low, shear. This was judged necessary as any detachment of the 322K polymer would be expected to occur at a rather low shear rate, given that the interanchor distance for this polymer−particularly in the presence of 182K chains—was expected to be large.

However, as can be seen in Figure 9 (adsorbance vs shear rate), no detachment at all occurred for low shear rates. On the contrary, at a shear rate of 9450 s^{-1} complete detachment of the adsorbed material was observed. The static reflectivity profile and the reflectivity spectrum measured after detachment of the 182K−322K system, together with corresponding volume fraction profiles, are shown in Figure 10.

Simultaneous detachment for the two components has also been observed in the case of 182K−239K bimodal system (see Table 2).

The above experimental facts lead to the conclusion that upon application of shear flow, desorption in the *bimodal* systems we have studied occurs in two discrete ways. When the

dx.doi.org/10.1021/ma401011f | *Macromolecules* 2013, 46, 6972−6980

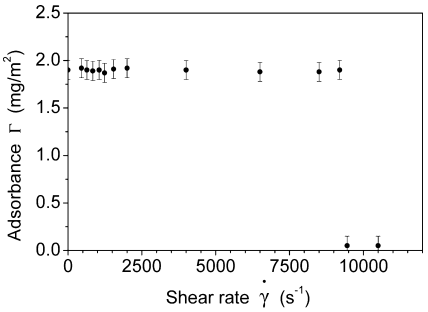

Figure 9. Adsorbance values of the 182K−322K PS−PEO bimodal brush system as a function of shear rate. No detachment occurs at low shear rate (below 1000 s^{-1}), which would be characteristic of desorption of the longer chains (322K). On the contrary, both molecular weights desorbed together at a shear rate of 9540 s^{-1}.

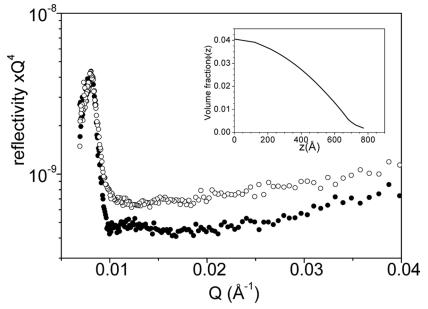

Figure 10. Reflectivity profiles of bimodal 182K−322K PS−PEO diblock copolymer brushes. Filled circles represent the measured static (zero shear) profile. Open circles indicate the profile after desorption. Both components of the brush were found to desorb together. Simultaneous detachment for the two components was observed at 9450 s^{-1}. Inset: volume fraction profile for 182K−322K PS−PEO bimodal brush system for the static (zero shear) profile.

PS brush height ratio of the components was less than 0.80, each component was desorbed at *different* shear rates, while for brush height ratios above this value desorption occurs at the *same* shear rate for both polymers. In other words, below this ratio value the components respond individually to the applied shear flow, while above it the bimodal system responds as a whole. As was mentioned above, below this value, reflectivity spectra of the bimodal brushes are best fitted by two parabolas. This suggests that when the system consists of two types of chains that extend to substantially different heights above the anchoring surface so that a distinguishable step exists in chain height, then the longer chains that protrude beyond the brush layer formed by the shorter chains protect the latter from the shear forces. This critical height ratio of 0.8 appears to imply that in such bimodal brushes the penetration depth of the shear flow amounts to less than 20% of the mixed brush height. If chain ends belonging to both components reside within this depth, then both chains desorb at the same shear rate. When the difference in chain heights is greater, however, the longer chains that protrude well beyond the brush layer of the shorter ones are the first to desorb.

Thus, for all the combinations of molecular weight pairs examined in our bimodal systems, six experimental points in the $\dot{\gamma}_c(s)$ curve have been obtained which on a log−log plot lie on a straight line with a slope of −2.86 ± 0.08, as can be seen in Figure 11. It is important to note that this slope is essentially identical to that obtained in our previous investigation with unimodal brushes. Indeed, as shown in Figure 12, the log−log

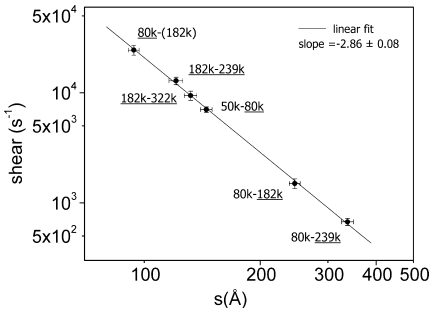

Figure 11. A log−log plot of critical shear rate, $\dot{\gamma}_c$, for chain detachment of bimodal brush systems versus interchain spacing, s, of polymeric chains that desorbed. The values of s and $\dot{\gamma}_c$ are presented in Table 2. Each experimental point is labeled with the molecular weight pair of the bimodal copolymer system that exposed to shear flow. In each case, the component of the bimodal system that detached at the critical shear rate is underlined. The linear fit of experimental points yields a slope of −2.86 ± 0.08, indicating that the power law $\dot{\gamma}_c \sim s^{-3}$ that was found previously for unimodal block copolymers[35] is also valid for bimodal systems.

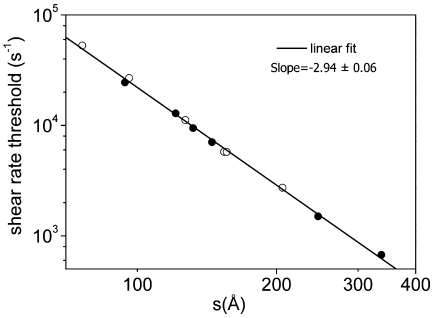

Figure 12. A log−log plot of critical shear rate, $\dot{\gamma}_c$, for chain detachment versus interchain spacing, s, for both unimodal block copolymer brushes[35] (open circles) and bimodal systems (full circles). The linear fit for both systems gives a slope of −2.94 (±0.06).

plot of critical shear rate $\dot{\gamma}_c$ for chain detachment versus interchain spacing s both for single block copolymers, i.e., unimodal brushes[35] (open circles) and bimodal systems (full circles) clearly demonstrates that both types of system are described by the same straight line with a slope of −2.94 ± 0.06.

These results indicate that the scaling law $\dot{\gamma}_c \sim s^{-3}$ that relates the critical shear rate for desorption to the interanchor spacing for both unimodal and bimodal PS brushes extends over a range of 2 decades in shear rate.

Brush Swelling near $\dot{\gamma}_c$. In 1991, a paper published by Klein et al.[36] reported that two brushes near contact exert additional normal forces when subjected to oscillatory shear above a certain shear velocity. This effect was interpreted as resulting from swelling of the brush under shear. Over the years numerous theoretical, experimental, and simulation studies seeking to establish such an effect ensued,[24−35,44,45] but to date no experiment aimed at *directly* probing the brush height under shear flow has demonstrated the existence of any measurable brush swelling. It is therefore of interest to examine our current results in this context.

In a previous work[35] we found no evidence of any brush swelling at shear rates right up to the onset of desorption at $\dot{\gamma}_c$. This observation is confirmed also in the present work, where no swelling of the constituent parts of our bimodal brush

dx.doi.org/10.1021/ma401011f | Macromolecules 2013, 46, 6972−6980

systems is detected just before desorption. This experimental fact is in agreement with the results of neutron reflectivity studies on similar systems.[9] In both our studies, i.e., the present work and ref 35, the region in the vicinity of $\dot{\gamma}_c$ was systematically investigated by measuring the reflectivity profile close to $\dot{\gamma}_c$, for a series of molecular weights and bimodal systems, in small steps of increasing shear rate, but no measurable change in the brush profile prior to desorption was ever detected. In order to address the issue of brush swelling, however, it is important to consider the sensitivity of the experimental technique employed in relation to the system under study. For the type of PS−PEO block copolymer brushes investigated in the present study as well as previously,[34,35] and within the Q-range that was accessible in our experiments, our neutron reflectivity measurements are capable of detecting changes in the brush volume fraction profile of as little as 10%. To illustrate this, we analyze the experimental reflectivity profiles, just below the critical shear rate for desorption, for two of our experimental data sets.

As an example we consider first the 182K−322K PS−PEO bimodal system (Figure 13) which shows no measurable

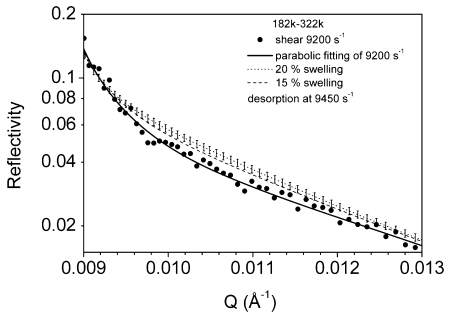

Figure 13. Neutron reflectivity profile of bimodal system 182K−322K PS−PEO block copolymer brush. This figure is an expanded version of Figure 10, in the Q-range 9×10^{-3}−1.3×10^{-2} Å^{-1}. Reflectivity measurements obtained in shear flow at a shear rate of 9200 s^{-1} (filled circles) are shown. The static measurements have been omitted as they are indistinguishable from their high-shear counterparts (9200 s^{-1}) within the scatter of the data points while the corresponding least-squares fits based on a parabolic density profile are identical (continuous line). The dashed and dotted curves indicate the calculated neutron reflectivity that would result from 15 and 20% swelling respectively of the static brush at fixed grafting density. The indicative error bars on the calculated swollen brush reflectivity profile (dotted line) are based on the same measurement statistics as those of the actual experimental points.

difference between the reflectivity profile at zero shear (static) and that measured at a shear rate of 9200 s^{-1}, this value being just below the critical shear rate, $\dot{\gamma}_c$, of 9450 s^{-1} where desorption occurs for this system. In other words, there is no evidence of any brush swelling at shear rates right up to the onset of desorption at $\dot{\gamma}_c$, under conditions where an effect of 15−20% brush swelling would be easily detectable by neutron reflectometry. This can be seen more clearly in an expanded version of Figure 10 (see Figure 13) to highlight the region where brush swelling effects would be most evident. In Figure 13, the reflectivity measurements obtained in shear flow at a shear rate of 9200 s^{-1} are shown together with the calculated neutron reflectivity that would result from a 15% and 20% swelling of the static brush at fixed grafting density indicated by the dashed and dotted curves, respectively. It is important to stress that the dashed reflectivity curve is ca. 15% higher than the measured reflectivity over a Q-range spanning numerous experimental points, while the error on the measured points is ca. ±4%. Consequently, a uniform swelling of the brush by 15% would be easily detectable in this experiment.

Figure 14 presents the corresponding volume fraction profiles whose neutron reflectivity curves are shown in Figure

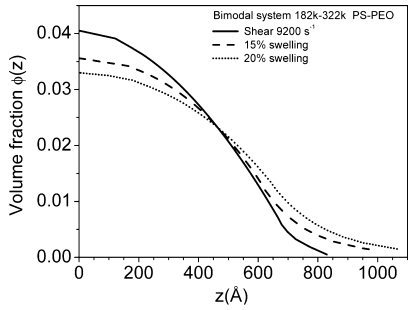

Figure 14. Volume fraction profiles for bimodal system 182K−322K whose neutron reflectivity is shown in Figure 13. The continuous line is obtained from the best fit parabolic profile to neutron reflectivity data just below the critical shear rate (9200 s^{-1}) shown in Figure 13. The dashed and dotted lines indicate the calculated volume fraction profile that would result from 15 and 20% swelling, respectively, of the static volume fraction profile at fixed grafting density. These profiles would give rise to the dashed and dotted reflectivity curves of Figure 13.

13 and demonstrates the difference between the static profile and a profile whose brush height has swollen by 15% (dashed curve) and 20% (dotted curve) under *fixed* grafting density. All profiles are parabolic with a Gaussian tail and the area under each curve is the same, but the brush heights of the swollen curves are 15% and 20% higher than that of the static profile. The continuous line is the profile for the polymer brush just before desorption, $\dot{\gamma}_c$ = 9200 s^{-1}, and the dashed and dotted lines describe the profiles that would result from a 15 and 20% swelling, respectively, of the static volume fraction profile at constant grafting density. The measured volume fraction profile at zero shear, however, is identical, within the experimental error, to that of $\dot{\gamma}_c$ = 9200 s^{-1}.

As a second example, we may consider Figure 1 of ref 35, which refers to the 80K PS−PEO block copolymer. Once again there is no measurable difference between the reflectivity profile at zero shear (static) and that measured at a shear rate of 4.99×10^4 s^{-1}, i.e., just below the critical shear rate, $\dot{\gamma}_c$, of 5.2×10^4 s^{-1}, where desorption occurs for this system. Specifically in this case because of the lower molecular weight and brush height of this polymer in comparison to the 182K−322K PS−PEO bimodal system, the reflectivity is even more sensitive to swelling. In an expanded version of Figure 1 of ref 35 (see Figure 15), both the static (zero shear) reflectivity measurements (open circles) and those obtained in shear flow at a shear rate of 4.99×10^4 s^{-1} (filled circles) are presented, together with the calculated neutron reflectivity that would result from a 10% swelling of the static brush at fixed grafting density indicated by the dashed curve. The dashed reflectivity curve is ca. 16% higher than the measured reflectivity over a Q-range spanning a large number of experimental points, whereas the error on the measured points is ca. ± 4%. This fact indicates that our neutron reflectivity measurements can easily detect a brush swelling of 10% for this particular polymer brush (i.e., PS−PEO 80K).

dx.doi.org/10.1021/ma401011f | *Macromolecules* 2013, 46, 6972−6980

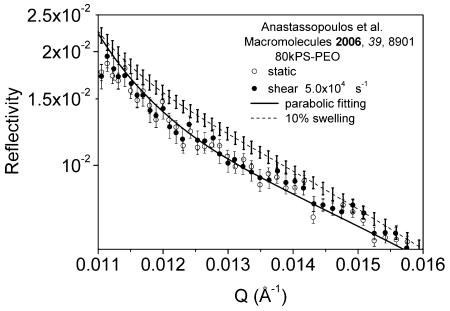

Figure 15. Neutron reflectivity profile of a hydrogenous polystyrene−poly(ethylene oxide) (PS−PEO) block copolymer brush of MW 80K, end-adsorbed onto quartz from *d*-toluene. The experimental points are neutron reflectivity measurements originally presented in Figure 1 of ref 35, but now expanded in the *Q*-range 1.1×10^{-2}−1.6×10^{-2} Å^{-1}. Both the static (zero shear) reflectivity measurements (open circles) and those obtained in shear flow at a shear rate of 4.99×10^4 s^{-1} (filled circles) are shown, together with the experimental error on each measured point. The static measurements are indistinguishable from their high-shear counterparts within the scatter of the data points while the corresponding least-squares fits based on a parabolic density profile are identical (continuous line). The dashed line indicates the calculated neutron reflectivity that would result from a 10% swelling of the static brush at fixed grafting density. The indicative error bars on the calculated swollen brush reflectivity profile (dashed line) are based on the same measurement statistics as those of the actual experimental points.

Figure 16 shows the volume fraction profiles that correspond to the neutron reflectivity curves presented in Figure 15 and

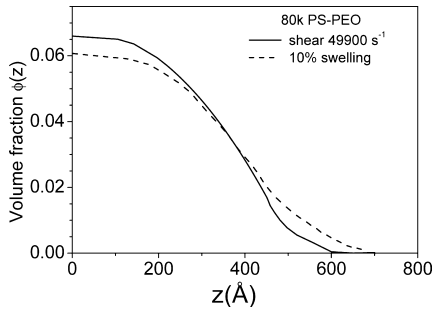

Figure 16. Volume fraction profiles for the polymer brush whose neutron reflectivity are shown in Figure 15. The continuous curve is obtained from the best fit parabolic profile to neutron reflectivity data just below the critical shear rate (4.99×10^4 s^{-1}) shown in Figure 15. There are very small, practically negligible differences between this fit and the best fit to the static neutron reflectivity data (see Figure 1 of ref 35) so the volume fraction profile corresponding to the latter is not shown for reasons of clarity. The dashed line indicates the calculated volume fraction profile that would result from a 10% swelling of the static volume fraction profile at fixed grafting density. This profile would give rise to the dashed reflectivity curve of Figure 15.

displays the difference between the static profile and a profile whose brush height has swollen by 10% under *fixed* grafting density. As before, both profiles are parabolic with a Gaussian tail and the area under both curves is the same, but the brush height of the curve corresponding to the swollen brush is 10% higher than its unswollen counterpart. The continuous line is the profile for the polymer brush just before desorption, at $\dot{\gamma}_c = 4.99 \times 10^4$ s^{-1}, and the dashed line depicts the profile that would result from a 10% swelling of the static volume fraction profile at constant grafting density. The experimentally determined volume fraction profile at zero shear, however, is indistinguishable from that of $\dot{\gamma}_c = 4.99 \times 10^4$ as was shown in Figure 1 of ref 35.

As noted in the present investigation and in our previous study (ref 35) the lack of change in the reflectivity profile just before the onset of desorption may suggest that the majority of chains remain essentially quiescent under strong shear flow leaving just a fraction of strongly extended chains to bear the brunt of the drag forces due to shear. This view appears to be supported by theory[31] and also by molecular dynamics simulations,[26] which show that only a small fraction of chains are strongly stretched under shear. It should be noted that the swelling predicted by the theory of Aubouy et al.[31] actually refers to such a small fraction of strongly extended chains. Such a picture would also be consistent with the well-known fact that the equilibrium free-end distribution of polymer chains in a brush is a very broad one,[18,42] which implies that the majority of chain ends remain buried within the brush layer. It is plausible that desorption of the chains at shear rates above the critical threshold is mediated by a very small fraction of highly stretched chains that cause an undetectably small change to the volume fraction profile of the brush prior to desorption.

In general, for the type of PS−PEO block copolymer brushes used in our studies, and depending on the particular properties of the brush (specifically the grafting density and the brush height) the *minimum* extent of brush swelling that can be detected by neutron reflectometry varies from 5% to 15%. Extending the *Q*-range of the measurements to higher values and measuring to higher neutron counts to reduce the statistical error would further increase the sensitivity of the measurements.

We conclude therefore that our neutron reflectivity measurements (ref 35 and the present work) are sensitive enough to detect brush swelling effects on the order of 10%. Consequently, our careful stepwise approach to the critical shear rate, i.e., right up to $\dot{\gamma}_c$, would identify a swelling of such a magnitude. Thus, our results indicate that any shear-induced brush swelling, if at all present, must amount to less than 10% change in the volume fraction profile of the brush.

CONCLUSIONS

In the present work we have performed an experimental study of the behavior of bimodal brushes in good solvent under shear flow.

We found that when, under static conditions, the chain height ratio of the bimodal brush components is lower than 0.80, then the reflectivity spectrum is best approximated by a double parabolic volume fraction profile. Above this ratio, however, the reflectivity spectrum can also be approximated by a single parabolic volume fraction profile with a tail.

When shear flow is applied, there is no measurable change in the reflectivity profile up to a certain shear rate threshold above which chain desorption takes place. Under conditions of shear flow, two discrete ways of desorption have been observed. When the chain height ratio of the bimodal brush components is below the critical value of 0.80, each component desorbs at a different shear rate, while for values above 0.80 desorption occurs at the same shear rate for both polymeric chains. This means that when the height of one kind of chain in the brush is significantly greater than the other, the longer chains desorb first, while if the heights of the two constituent kinds of chain in the brush are similar, then the bimodal system responds as a whole and both kinds of chain desorb simultaneously. All

dx.doi.org/10.1021/ma401011f | *Macromolecules* 2013, 46, 6972−6980

observed desorption behavior is found to obey a power law whereby the critical shear rate for desorption scales with s^{-3}, where s is the mean interanchor distance. This behavior has been previously confirmed for monodispersed brushes.[35] We have further confirmed the observation of our earlier experiments that there is no detectable brush swelling at shear rates right up to the onset of desorption at $\dot{\gamma}_c$. Our results, therefore, do not support the idea of brush expansion under shear, originally proposed by Klein et al.[36]

Our findings demonstrate the effect of bimodality on the response of polymer brushes to shear flow and may have potential technological utility in a range of applications.

AUTHOR INFORMATION

Corresponding Author

*E-mail: ctop@physics.upatras.gr (C.T.).

Notes

The authors declare no competing financial interest.

REFERENCES

(1) Napper, D. H. *Polymeric Stabilization of Colloidal Dispersions*; Academic Press: London, 1983.
(2) Fleer, G. J.; Cohen Stuart, M. A.; Scheutjens, J. M. H. M.; Cosgrove, T.; Vincent, B. *Polymers at Interfaces*; Chapman & Hall: Bristol, UK, 1993.
(3) Advincula, R. C., Brittain,W. J., Caster, K. C., Ruhe, J., Eds.; *Polymer Brushes: Synthesis, Characterization, Applications*; Wiley: Hoboken, NJ, 2004.
(4) Brittain, W. J.; Minko, S. *J. Polym. Sci., Part A: Polym. Chem.* **2007**, *45*, 3505−3512.
(5) Alexander, S. *J. Phys. (Paris)* **1977**, *38*, 983−986.
(6) De Gennes, P. G. *Adv. Colloid Interface Sci.* **1987**, *27*, 189−209.
(7) Hadziioannou, G.; Patel, S.; Granick, S.; Tirrell, M. *J. Am. Chem. Soc.* **1986**, *108*, 2869−2876.
(8) Field, J. B.; Toprakcioglu, C.; Ball, R. C.; Stanley, H. B.; Dai, L.; Barford, W.; Penfold, J.; Smith, G.; Hamilton, W. *Macromolecules* **1992**, *25*, 434−439.
(9) Ivkov, R.; Butler, P. D.; Satijia, S. K.; Fetters, L. J. *Langmuir* **2001**, *17*, 2999−3005.
(10) Hamilton, W.A.; Smith, G. S.; Alcantar, N. A.; Majewski, J.; Kuhl, T. L. *J. Polym. Sci., Part B: Polym. Phys.* **2004**, *42*, 3290−3301.
(11) Taunton, H. J.; Toprakcioglu, C.; Fetters, L. J.; Klein, J. *Macromolecules* **1990**, *23*, 571−580.
(12) Halperin, A.; Tirrell, M.; Lodge, T. P. *Adv. Polym. Sci.* **1992**, *100*, 31−71.
(13) Patel, S.; Tirrell, M. *Annu. Rev. Phys. Chem.* **1989**, *40*, 597−635.
(14) Grest, G. S.; Murat, M. *Computer Simulations of Tethered Chains. Monte Carlo and Molecular Dynamics Simulations in Polymer Science*; Binder, K., Ed.; Clarendon Press: Oxford, 1994.
(15) Szleifer, I.; Carignano, M. A. *Adv. Chem. Phys.* **1996**, *94*, 165−260.
(16) Minko, S. *J. Macromol. Sci., Part C: Polym. Rev.* **2006**, *46*, 397−420.
(17) Milner, S. T.; Witten, T. A.; Cates, M. E. *Europhys. Lett.* **1988**, *5*, 413−418.
(18) Milner, S. T.; Witten, T. A.; Cates, M. *Macromolecules* **1989**, *22*, 853−861.
(19) Birshtein, T. M.; Liatskaya, Y. V.; Zhulina, E. B. *Polymer* **1990**, *31*, 2185−2196.
(20) Dan, N.; Tirrell, M. *Macromolecules* **1993**, *26*, 6467−6473.
(21) Chakrabarti, A.; Toral, R. *Macromolecules* **1990**, *23*, 2016−2021.
(22) Chen, H.; Chakrabarti, A. *Phys. Rev. E* **1995**, *52*, 3915−3922.
(23) Kent, M. S.; Factor, B. J.; Satija, S.; Gallagher, P.; Smith, G. S. *Macromolecules* **1996**, *29*, 2843−2849.
(24) Rabin, Y.; Alexander, S. *Europhys. Lett.* **1990**, *13*, 49−54.
(25) Miao, L.; Guo, H.; Zuckermann, M. *Macromolecules* **1996**, *29*, 2289−2297.
(26) Grest, G. S. *Adv. Polym. Sci.* **1999**, *138*, 149−183.
(27) Lai, P. Y.; Binder, K. *J. Chem. Phys.* **1993**, *98*, 2366−2375.
(28) Barrat, J. L. *Macromolecules* **1992**, *25*, 832−834.
(29) Kumaran, V. *Macromolecules* **1993**, *26*, 2464−2469.
(30) Harden, J. L.; Cates, M. E. *Phys. Rev. E* **1996**, *53*, 3782−3787.
(31) Aubouy, M.; Harden, J. L.; Cates, M. E. *J. Phys. II* **1996**, *6*, 969−984.
(32) Doyle, P. S.; Shaqfeh, E. S. G.; Gast, A. P. *Phys. Rev. Lett.* **1997**, *78*, 1182−1185.
(33) Saphiannikova, M. G.; Pryamitsyn, V. A.; Cosgrove, T. *Macromolecules* **1998**, *31*, 6662−6668.
(34) Baker, S. M.; Smith, G.; Anastassopoulos, D. L.; Toprakcioglu, C.; Vradis, A. A.; Bucknall, D. G. *Macromolecules* **2000**, *33*, 1120−1122.
(35) Anastassopoulos, D. L.; Spiliopoulos, N.; Vradis, A. A.; Toprakcioglu, C.; Baker, S. M.; Menelle, A. *Macromolecules* **2006**, *39*, 8901−8904.
(36) Klein, J.; Perahia, D.; Warbourg, S. *Nature (London)* **1991**, *352*, 143−145.
(37) Klein, J. *Pure Appl. Chem.* **1992**, *64*, 1577−1584.
(38) Saphiannikova, M. G.; Pryamitsyn, V. A.; Birshtein, T. M. *Macromolecules* **2000**, *33*, 2740−2747.
(39) Baker, S. M.; Smith, G.; Pynn, R.; Butler, P.; Hayter, J.; Hamilton, W.; Magid, L. *Rev. Sci. Instrum.* **1994**, *85*, 412−416.
(40) Battaglin, G.; Menelle, A.; Montecchi, M.; Nichelatti, E.; Polato, P. *Glass Technol.* **2002**, *43*, 203−208.
(41) Hiotelis, I.; Koutsioubas, A. G.; Spiliopoulos, N.; Anastassopoulos, D. L.; Vradis, A. A.; Toprakcioglu, C.; Menelle, A.; Sakellariou, G.; Hadjichristidis, N. *Macromolecules* **2008**, *41*, 7648−7655.
(42) Spiliopoulos, N.; Koutsioubas, A. G.; Anastassopoulos, D. L.; Vradis, A. A.; Toprakcioglu, C.; Menelle, A.; Mountrichas, G.; Pispas, S. *Macromolecules* **2009**, *42*, 6209−6214.
(43) Russell, T. P. *Mater. Sci. Rep.* **1990**, *5*, 171−271.
(44) Eiser, E.; Klein, J. *Macromolecules* **2007**, *40*, 8455−8463.
(45) Ji, S.; Ding, J. *J. Chem. Phys.* **2005**, *123*, 144904.